

Article

Protective Effect of N-Acetylcysteine against Oxidative Stress Induced by Zearalenone via Mitochondrial Apoptosis Pathway in SIEC02 Cells

Jingjing Wang [†], Mengmeng Li [†], Wei Zhang, Aixin Gu, Jiawen Dong, Jianping Li ^{*†} 
and Anshan Shan ^{*}

Institute of Animal Nutrition, Northeast Agricultural University, Harbin 150030, China; JF_JING@hotmail.com (J.W.); limengmeng@outlook.com (M.L.); zhangwei910315@hotmail.com (W.Z.); aixingu@hotmail.com (A.G.); dongjiawen2018@outlook.com (J.D.)

^{*} Correspondence: ljpnneau@gmail.com (J.L.); asshan@neau.edu.cn (A.S.); Tel.: +86-0451-5519-1439 (J.L.)

[†] These authors contributed equally to the paper.

Received: 5 August 2018; Accepted: 2 October 2018; Published: 9 October 2018



Abstract: Zearalenone (ZEN), a nonsteroidal estrogen mycotoxin, is widely found in feed and foodstuffs. Intestinal cells may become the primary target of toxin attack after ingesting food containing ZEN. Porcine small intestinal epithelial (SIEC02) cells were selected to assess the effect of ZEN exposure on the intestine. Cells were exposed to ZEN (20 µg/mL) or pretreated with (81, 162, and 324 µg/mL) N-acetylcysteine (NAC) prior to ZEN treatment. Results indicated that the activities of glutathione peroxidase (Gpx) and glutathione reductase (GR) were reduced by ZEN, which induced reactive oxygen species (ROS) and malondialdehyde (MDA) production. Moreover, these activities increased apoptosis and mitochondrial membrane potential ($\Delta\Psi_m$), and regulated the messenger RNA (mRNA) expression of Bax, Bcl-2, caspase-3, caspase-9, and cytochrome c (cyto c). Additionally, NAC pretreatment reduced the oxidative damage and inhibited the apoptosis induced by ZEN. It can be concluded that ZEN-induced oxidative stress and damage may further induce mitochondrial apoptosis, and pretreatment of NAC can degrade this damage to some extent.

Keywords: Zearalenone; N-acetylcysteine; SIEC02 cells; Mitochondrial apoptosis

Key Contribution: The gastrointestinal tract is the primary target of mycotoxin attack, and ZEN produced cytotoxic effects on SIEC02 cells. Oxidative stress and mitochondrial apoptosis of SIEC02 cells, produced after exposure to ZEN and NAC pretreatment, can alleviate the negative effect of ZEN on SIEC02 cells.

1. Introduction

Zearalenone (ZEN), a secondary metabolite produced by fungi of the genus *Fusarium*, can seriously affect animal growth, reproduction, and immune function [1–3]. Studies estimate that one-fourth of the global food and feed output is contaminated by mycotoxins, and the number is likely to be closer to 50% if new fungal toxins are considered for limited data [4,5]. ZEN is being increasingly recognized as a frequent contaminant in animal feeding, which has a significant effect on human and animal health [6,7]. According to a recent report, the United States Department of Agriculture (USDA), the European Food Safety Authority (EFSA), and China are concerned about mycotoxin contamination in cereals, and they have renewed the maximum residue limits (MRLs) in food and feeds [8]. The MRLs in food is 350 µg/kg, 350 µg/kg, and 60 µg/kg, respectively. EFSA and China also reiterated that the MRLs in feed is 2000 µg/kg and 500 µg/kg [8].

It is shown that most animals have a certain sensitivity to ZEN, and the pig is the most sensitive animal [9]. The primary attack target of toxins from ingested food or feed is the gastrointestinal tract, and thus it affects intestinal function [10,11]. The main metabolites of ZEN are α -zearalenol (α -ZOL) and β -zearalenol (β -ZOL) [12]. Establishing a barrier model (IPEC-1) in vitro, study has shown that ZEN and its metabolites damage barrier function by reducing the immune response [13]. It has been reported that ZEN affects the villous structures and reduces the expression of junction proteins in a dose-dependent manner in pregnant rats [14]. The estrogen-like effects of ZEN and its derivatives have been determined in vivo and in vitro [13,15]. A further experiment has demonstrated that oxidative damage is likely to be evoked as one of the main pathways of ZEN toxicity [16]. Moreover, data suggested that ZEN induced apoptosis in a dose-dependent manner in many cell lines (HepG2, porcine granulosa, and SHSY-5Y cells) [6,17,18]. Therefore, it is necessary to analyze the effect of ZEN on the intestinal tract.

N-acetylcysteine (NAC), the precursor of glutathione, is a water-soluble molecule that has antioxidant, anti-inflammatory, and tumor-inhibitory properties [19,20]. A previous study has shown that NAC can exert antioxidant effects both in vitro and in vivo [21]. It is generally assumed that the action of NAC is to scavenge free radicals by increasing the intracellular glutathione (GSH) level [22]. More recently, studies have found that NAC can directly inhibit the production of reactive oxygen species (ROS), and thus inhibit apoptosis [23,24]. Similarly, NAC pretreatment can reduce lipid peroxidation and inhibit apoptosis [25]. In addition, NAC also plays an important role in protecting renal function by reducing oxidative stress [26,27].

Cells were poisoned by ZEN, cells may undergo complex and different pathways of damage, including apoptosis [16,18]. The SIEC02 cells retained the morphological and functional characteristics that were typical of primary swine intestinal epithelial cells by introducing the human telomerase reverse transcriptase, and thus they provide a cell model in vitro [28]. However, the mechanism underlying the apoptosis of intestinal cells after exposure to ZEN is still not totally understood. Therefore, the purpose of this study was to evaluate whether ZEN-induced oxidative damage could further lead to apoptosis, and whether the addition of NAC could alleviate this negative effect on SIEC02 cells.

2. Results

2.1. Effects of ZEN and NAC on Cell Viability

To examine the cytotoxic effects of ZEN, SIEC02 cells were incubated with ZEN (5, 10, 15, 20, 25 and 30 $\mu\text{g}/\text{mL}$) for 24 h. After incubation, ZEN treatment inhibited the cell viability markedly in a dose-dependent manner (Figure 1A). Cell viability was only 36.30% at a ZEN concentration of 30 $\mu\text{g}/\text{mL}$, and the inhibitory concentration of IC_{50} (50% inhibitory concentration) was $22.68 \pm 0.80 \mu\text{g}/\text{mL}$. Hence, a cytotoxic concentration of ZEN (20 $\mu\text{g}/\text{mL}$) was selected for subsequent experiments. In addition, NAC alone did not show any cytotoxicity at concentrations (81, 162, and 324 $\mu\text{g}/\text{mL}$) of incubation for 6 h. However, compared with the control group, cell viability was significantly reduced when cells were treated by NAC (162 and 324 $\mu\text{g}/\text{mL}$) for 12 h ($P < 0.05$). All three concentrations of NAC significantly reduced cell viability for 24 h ($P < 0.01$) (Figure 1B). Based on the additions shown in Figure 1B, NAC concentrations (81, 162 and 324 $\mu\text{g}/\text{mL}$) were selected for pretreating the cells for 6 h prior to the ZEN treatment.

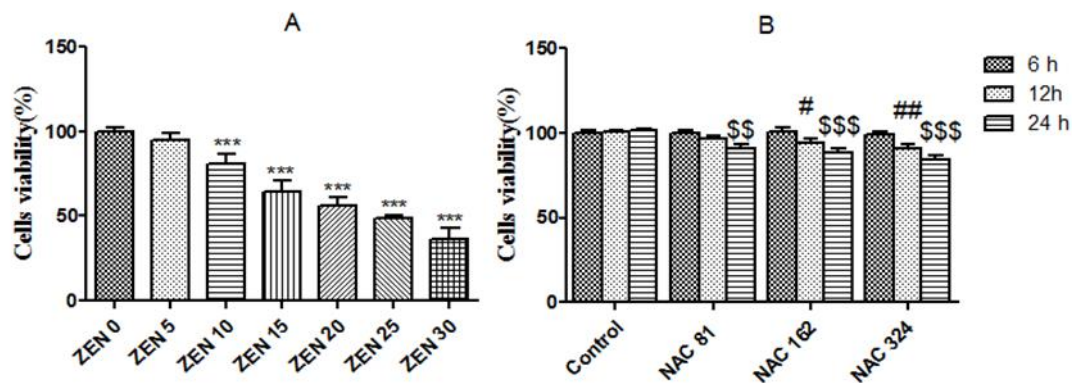


Figure 1. Effects of zearalenone (ZEN) and N-acetylcysteine (NAC) on SIEC02 cells viability. Cells were treated without or with different concentrations of ZEN (0, 5, 10, 15, 20, 25 and 30 µg/mL) for 24 h (A). Cells were pretreated without or with different concentrations of NAC (81, 162 and 324 µg/mL) for 6 h, 12 h, and 24 h (B). Cells survival was measured by Cell Counting Kit-8 (CCK-8) assay. The values are mean \pm SD of three independent experiments. *** indicates a significant difference between ZEN and control at $P < 0.001$. #, ## indicates a significant difference of 12 h between NAC and control, with significant differences at $P < 0.05$ and $P < 0.01$. \$\$, \$\$\$ indicates a significant difference of 24 h between NAC and the control at $P < 0.01$ and $P < 0.001$.

2.2. Effects of ZEN and NAC on Oxidative Stress

2.2.1. Glutathione peroxidase (Gpx) Activity

Data on the activity of antioxidative enzymes and related products in SIEC02 cells is summarized in Figure 2. As shown in Figure 2A, Gpx activity was significantly reduced after ZEN treatment on 0.227 µmol/mg of protein, compared with the control group (0.325 µmol/mg) ($P < 0.001$). The Gpx activity was restored to a certain extend by the pretreatment of cells with NAC (81, 162 and 324 µg/mL) ($P < 0.001$) and increased to 0.247, 0.248 and 0.254 µmol/mg of protein, respectively. Based on these data, NAC pretreatment could significantly increase the reduction in Gpx activity induced by ZEN, and the optimal concentration of NAC was 324 µg/mL ($P < 0.05$).

2.2.2. Glutathione reductase (GR) Activity

According to Figure 2B, compared with the control group (11.307 U/mg), the GR activity of ZEN treatment was significantly reduced to 0.857 U/mg of protein ($P < 0.001$). The reduction in GR activity induced by ZEN was restored to a certain extend by the treatment of cells with NAC (81, 162 and 324 µg/mL) ($P < 0.05$) and increased to 3.859, 3.537 and 3.269 U/mg of protein, respectively. Based on these data, NAC pretreatment could significantly increase the activity of GR. Three concentrations of NAC did not reach a significant level.

2.2.3. Malondialdehyde (MDA) Level

As shown in Figure 2C, the MDA level of ZEN treatment was significantly higher (151.9 nmol/mg of protein) than the control group (32.2 nmol/mg) ($P < 0.001$). Pretreatment with NAC (81, 162 and 324 µg/mL) significantly reduced the increase in the MDA level as induced by ZEN ($P < 0.001$), and decreased to 132.2, 130.2 and 132.5 nmol/mg of protein, respectively. Three concentrations of NAC did not reach a significant level.

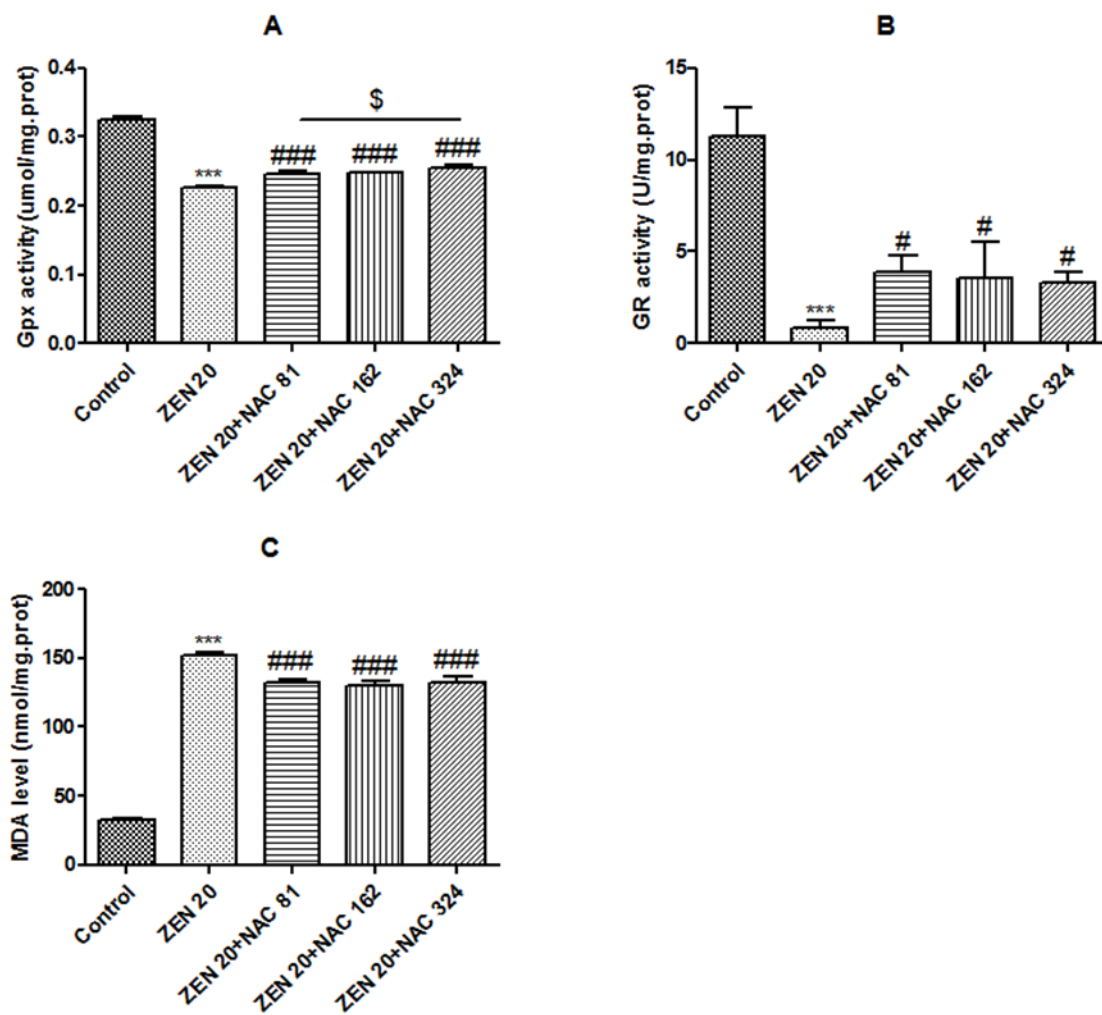


Figure 2. Effect of ZEN (20 µg/mL) and NAC (81, 162 and 324 µg/mL) on intracellular glutathione peroxidase (Gpx), glutathione reductase (GR) activity, and malondialdehyde (MDA) levels. Cells were exposed to ZEN for 24 h, including NAC pretreatment for 6 h. The results of Gpx, GR, and MDA were µmol/mg, U/mg, nmol/mg of protein, respectively. Each set of data shows the mean ± SD of three independent experiments. *** indicates a significant difference between ZEN and control $P < 0.001$. #, ###, indicates a significant difference between ZEN and NAC in mutual treatment at $P < 0.05$ and $P < 0.001$. \$ indicates a significant difference between three concentrations of NAC at $P < 0.05$ (A–C).

2.3. Effects of ZEN and NAC on Intracellular ROS Generation

ROS was generated as by-products of cellular metabolism, which could trigger oxidative stress at high concentrations [29]. ROS production was monitored by measuring the fluorescence intensity of DCFH-DA (2',7'-dichlorodihydrofluorescein diacetate dye). DCFH-DA is a fluorescent probe of ROS. The non-fluorescent fluorescein DCFH-DA derivatives will emit fluorescence after being oxidized by the radicals generated by the toxins. In the presence of ROS, H_2 -DCF is rapidly oxidized to become highly fluorescent DCF [30,31]. The result indicated that ZEN could significantly induce ROS accumulation in SIEC02 cells ($P < 0.001$) (Figure 3) and the ROS content in the ZEN group was significantly higher than that in control group. As observed in Figure 3, NAC pretreatment significantly reduced ZEN-induced ROS production ($P < 0.01$), and the optimal concentration of NAC was 162 µg/mL ($P < 0.05$).

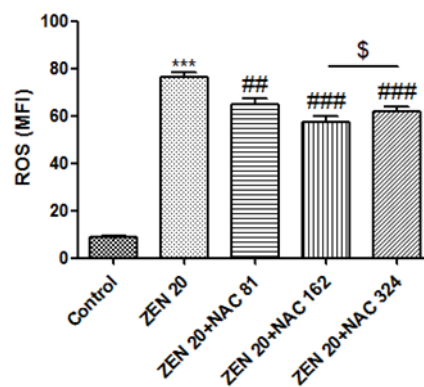


Figure 3. Effect of ZEN (20 $\mu\text{g}/\text{mL}$) and NAC (81, 162 and 324 $\mu\text{g}/\text{mL}$) on intracellular reactive oxygen species (ROS) production. Cells were exposed to ZEN for 24 h, including NAC pretreatment for 6 h. The results are expressed as mean fluorescent intensity (MFI). Each set of data shows the mean \pm SD of the three independent experiments. *** indicates a significant difference between ZEN and control at $P < 0.001$. ##, ### indicates a significant difference between ZEN and NAC in mutual treatment at $P < 0.01$ and $P < 0.001$. \$ indicates a significant difference between three concentrations of NAC at $P < 0.05$.

2.4. Effects of ZEN and NAC on Apoptosis

Cells were stained with Annexin V-FITC/PI to determine whether ZEN induced cell apoptosis and its consequences following alleviation with NAC were evaluated. Compared with the control group (Figure 4A), the number of living cells were decreased and the early apoptosis of ZEN treatment, and the late apoptotic cells were significantly increased ($P < 0.05$) (Figure 4B and 4F). As seen in Figure 4C,D,E and F, the apoptotic cells of Q2 and Q4 were reduced compared with Figure 4B, and the apoptotic rate was also significantly reduced ($P < 0.01$) by NAC pretreatment. The optimal concentration of NAC was 324 $\mu\text{g}/\text{mL}$ ($P < 0.05$) (Figure 4F).

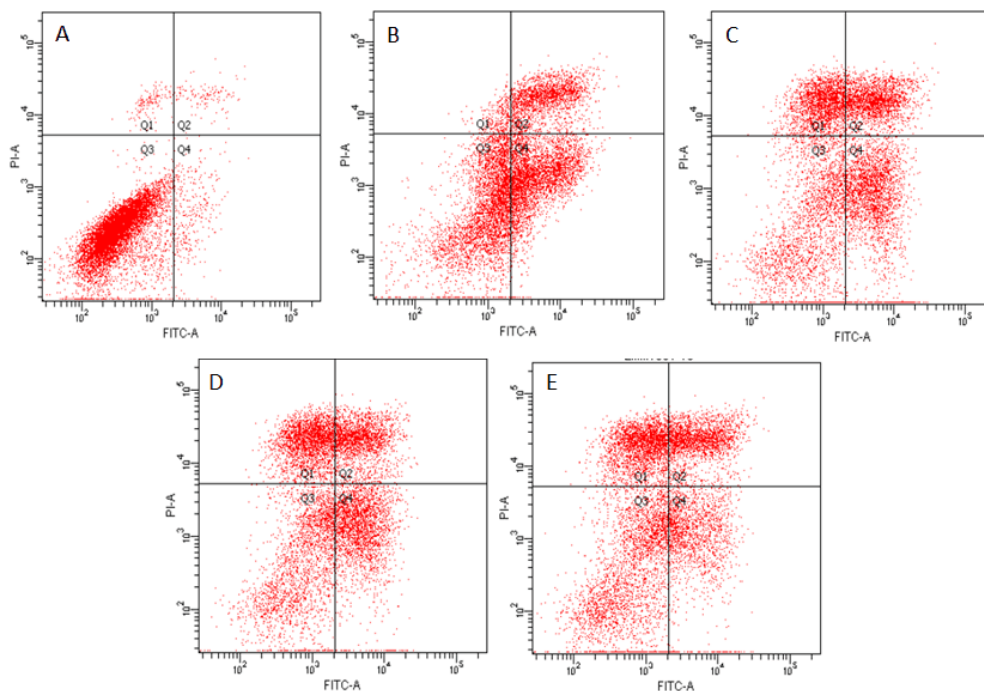


Figure 4. Cont.

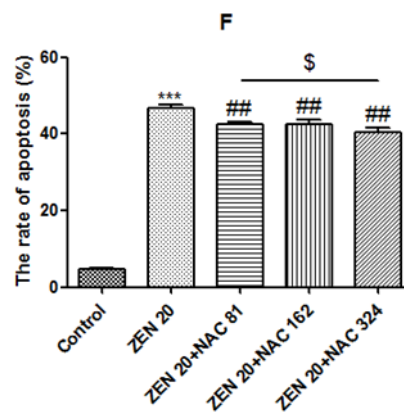


Figure 4. Annexin V-FITC/PI flow cytometry was used to detect SIEC02 cells treated with ZEN (20 µg/mL) and NAC (81, 162 and 324 µg/mL). The Q1, Q2, Q3, and Q4 gates, respectively, represented dead cells, the late stage of cell apoptosis, normal cells, and the early stage of cell apoptosis (A, B, C, D and E are control, ZEN 20 µg/mL, ZEN 20 µg/mL + NAC 81 µg/mL, ZEN 20 µg/mL + NAC 162 µg/mL, and ZEN 20 µg/mL + NAC 324 µg/mL, respectively). Apoptosis results are expressed as the rate of apoptosis. Each set of data shows the mean \pm SD of the three independent experiments. *** indicates a significant difference between ZEN and control at $P < 0.001$. ## indicates a significant difference between ZEN and NAC in mutual treatment at $P < 0.01$. \$ indicates a significant difference between three concentrations of NAC at $P < 0.05$ (F).

2.5. Effects of ZEN and NAC on the Change of $\Delta\Psi_m$

JC-1 (mitochondrial probe) formed J-aggregates in the mitochondrial matrix (red) at high $\Delta\Psi_m$ in nonapoptotic cells, and formed monomeric (green) at low $\Delta\Psi_m$ in apoptotic cells (Figure 5). Therefore, the change of $\Delta\Psi_m$ was reflected by decreasing the red and green fluorescence ratio. The effects of different treatments on mitochondrial membrane potential in SIEC02 cells are shown in Figure 5A–E. As shown in Figure 5B, the green aggregates were increased compared with the control group (Figure 5A), indicating that the $\Delta\Psi_m$ was decreased, the cell membrane was severely damaged, and the apoptosis rate was significantly increased ($P < 0.001$) (Figure 5F). After NAC pretreatment, green aggregates showed signs of weakening (Figure 5C,D and E) compared with the ZEN group (Figure 5B). The apoptosis rate of the cells was significantly decreased by NAC pretreatment ($P < 0.01$) and it did not reach a significant level in the three concentrations of NAC (Figure 5F).

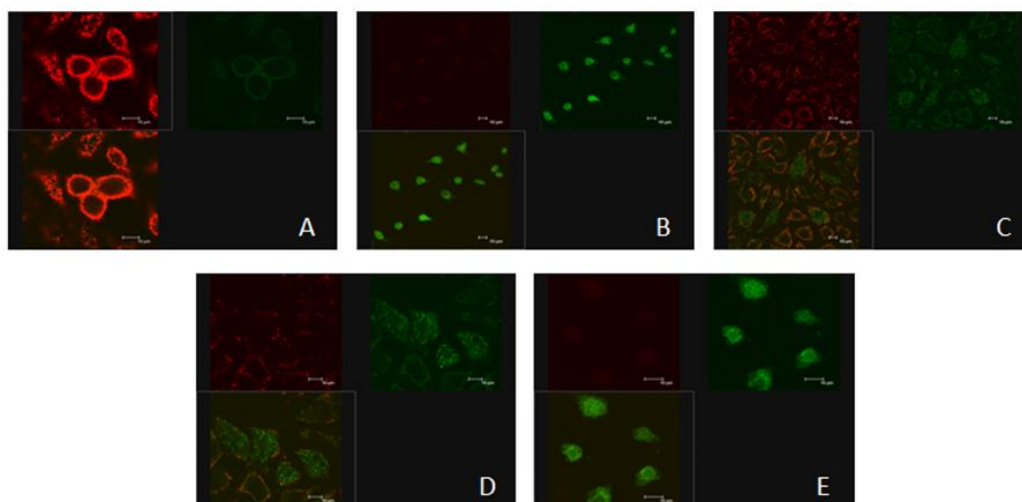


Figure 5. Cont.

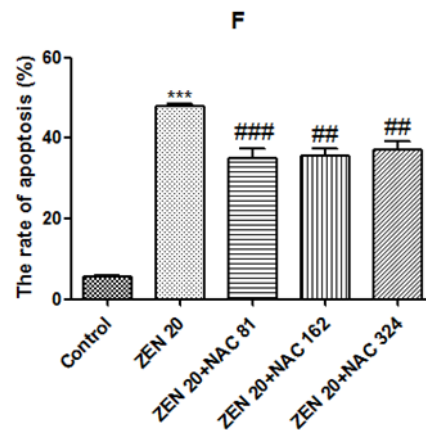


Figure 5. A laser scanning confocal microscope was used to observe the changes of mitochondrial membrane potential ($\Delta\Psi_m$) in SIEC02 cells treated with ZEN and NAC. The scanning pictures were as shown in the figure (A–E are control, ZEN 20 $\mu\text{g}/\text{mL}$, ZEN 20 $\mu\text{g}/\text{mL}$ + NAC 81 $\mu\text{g}/\text{mL}$, ZEN 20 $\mu\text{g}/\text{mL}$ + NAC 162 $\mu\text{g}/\text{mL}$ and ZEN 20 $\mu\text{g}/\text{mL}$ + NAC 324 $\mu\text{g}/\text{mL}$, respectively). Scale bar: 10 μm . The results are expressed as apoptosis rate (F); each set of data shows the mean \pm SD of the three independent experiments. *** indicates a significant difference between ZEN and control at $P < 0.001$. ##, ### indicates a significant difference between ZEN and NAC in mutual treatment at $P < 0.01$ and $P < 0.001$ (F).

2.6. Effects of ZEN and NAC on Apoptosis-Related mRNA Expression

2.6.1. Bax

The effects of ZEN and NAC protection apoptosis-related mRNA levels via caspase pathways are shown in Figure 6. As shown in Figure 6A, the mRNA expression levels of Bax were significantly increased by ZEN, compared with the control group ($P < 0.001$). Compared with the ZEN treatment, the NAC-pretreated significantly reduced the mRNA expression of Bax ($P < 0.001$). Three concentrations of NAC did not reach a significant level.

2.6.2. Bcl-2

The expression of Bcl-2 mRNA was opposite to that of Bax. As shown in Figure 6B, the mRNA expression levels of Bax were significantly decreased in the ZEN group ($P < 0.01$). Compared with ZEN treatment, the production of Bcl-2 could not be significantly decreased at a NAC concentration of 324 $\mu\text{g}/\text{mL}$. When the concentration of NAC were 81 and 162 $\mu\text{g}/\text{mL}$, the mRNA expression of Bcl-2 significantly increased ($P < 0.001$), and the optimal concentration of NAC was 162 $\mu\text{g}/\text{mL}$ ($P < 0.01$).

2.6.3. Cytochrome c (Cyto c)

As shown in Figure 6C, the mRNA expression levels of cyto c were significantly increased by ZEN ($P < 0.01$). Compared with ZEN treatment, the production of cyto c could not be significantly decreased at a NAC concentration of 81 $\mu\text{g}/\text{mL}$. When the NAC concentration of NAC were 162 and 324 $\mu\text{g}/\text{mL}$, cyto-c production was significantly decreased ($P < 0.01$).

2.6.4. Caspase-9 and Caspase-3

Similar to cyto c mRNA expression, caspase-9 and caspase-3 mRNA levels were significantly increased by ZEN ($P < 0.05$) (Figure 6D,E). Compared with ZEN treatment, the mRNA expression of caspase-9 was significantly reduced at the NAC concentrations of 81 and 162 $\mu\text{g}/\text{mL}$ ($P < 0.05$). At the same time, when the NAC concentration of NAC were 162 and 324 $\mu\text{g}/\text{mL}$, the mRNA expression of caspase-3 was significantly increased ($P < 0.001$).

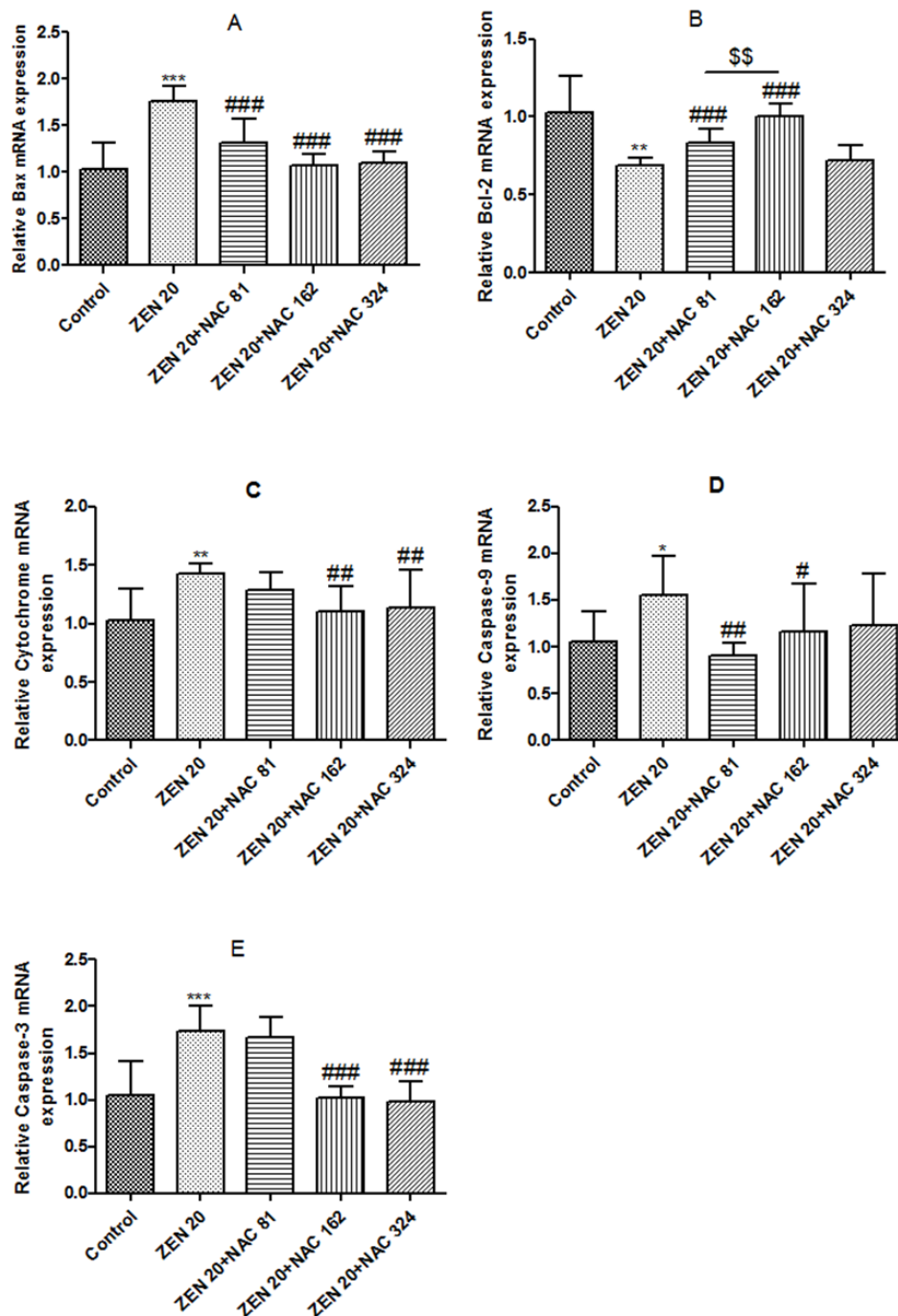


Figure 6. The results of the ZEN (20 $\mu\text{g}/\text{mL}$) and NAC (81, 162 and 324 $\mu\text{g}/\text{mL}$) expression levels of each apoptotic gene (Bcl-2, Bax, cytochrome c, caspase-9, caspase-3) in the SIEC02 cells. Cells were exposed to ZEN for 24 h, including NAC pretreatment for 6 h. The results are expressed relative to the expression of actin; each set of data shows the mean \pm SD of the three independent experiments. *, **, *** indicates a significant difference between ZEN and control at $P < 0.05$, $P < 0.01$, and $P < 0.001$. #, ##, ### indicates a significant difference between ZEN and NAC in mutual treatment at $P < 0.05$, $P < 0.01$, and $P < 0.001$. \$\$ indicates a significant difference between three concentrations of NAC at $P < 0.01$ (A–E).

3. Discussion

ZEN and its major metabolites are secondary metabolites of *Fusarium* fungi that produce cell damage [12,32]. A number of studies have found that ZEN has an inhibitory effect on cell proliferation [15,16]. The most direct indicator is the number of living cells due to toxic changes.

The IC_{50} is an important indicator of the cellular response to chemical effects. In human hepatoma cells (HepG2) and colorectal cancer cells (HCT116), the IC_{50} is 100 μ M and 60 μ M, respectively, and cell proliferation undergoes a dose-dependent reduction after ZEN treatment [18,33]. In this experiment, Cell Counting Kit-8 (CCK-8) method was used to detect the effect of ZEN on the activity of SIEC02 cells cultured in vitro. The results showed that after treatment with ZEN for 24 h, the IC_{50} range was 22.68 ± 0.80 μ g/mL (62.89 μ M). This value might differ slightly from that just mentioned, because of differences in cell lines. With the increase in ZEN concentration, the cell activity gradually decreased and showed a dose-response relationship.

The gastrointestinal tract is the primary site of toxin interaction, and intestinal epithelial cells are an important first target site for mycotoxin [34,35]. Most studies of toxicity have shown that the cytotoxicity of ZEN is determined by the production of ROS, DNA damage, and an increased formation of lipid peroxidation [36,37]. In normal physiological processes, small amounts of ROS are generated as by-products of cellular metabolism, primarily in the mitochondria [29,32]. ROS are highly reactive molecules, among which oxygen-free radicals can destroy cell structures, and increase lipid peroxidation of biofilms [38,39]. MDA, as the final product of lipid peroxidation, which can cause cell serious injuries in membrane structure, changes the permeability of cell membranes, leading to cell apoptosis, and necrosis [40]. Therefore, the measurement of MDA content can indirectly reflect the degree of lipid peroxidation. In this experiment, our results showed that 20 μ g/mL of ZEN significantly increased ROS and MDA contents in SIEC02 cells. Previous studies have found similar effects in different cell types that are exposed to ZEN. These results were consistent with the findings that ZEN can significantly increase ROS in CHO-K1 and IPEC-J2 cells and MDA in Caco-2 cells [36,41,42].

NAC, a precursor of GSH that is a free radical scavenger, which plays an important role as an antagonistic foreign chemical to the oxidative damage caused by biological organisms [22,43]. The antioxidant activity of NAC is evaluated by the enzymatic system. The antioxidant enzymes and other regulatory enzymes can be used as the first line of defense, and they play a role in scavenging free radical damage intracellularly and extracellularly [38]. GR and Gpx are the intrinsic anti-oxidative enzymes of cells [44]. Gpx catalyzes GSH to decompose H_2O_2 into water, and to form Glutathione oxidized (GSSG), and the GR enzyme can reduce GSSG to GSH, to scavenge excess H_2O_2 [45,46]. NAC could increase intracellular glutathione and produce sulfhydryl groups that directly eliminate ROS, such as hypochlorous acid, hydrogen peroxide, superoxide, and hydroxyl radicals [47,48]. Consequently, NAC increases the activity of the antioxidant enzymes Gpx and GR by restoring intracellular GSH content, thereby eliminating ROS. In this experiment, our data clearly demonstrated that the activities of Gpx and GR were significantly increased after NAC pretreatment, and that ROS was significantly reduced. Our study showed that NAC preconditioning could alleviate the activity of antioxidant enzymes in SIEC02 cells, and this result is also consistent with another team's results on the pig kidney PK15 cells [49]. In addition, pretreatment with NAC positively reduced ROS generation, suggesting a potential antioxidant for NAC, which is conformed to reduce cellular ROS by adding NAC in Jurkat T cells [50].

Apoptosis, a form of programmed cell death, is an essential process in cell growth, reproduction, and self-adjustment and it is characterized by morphological changes such as nucleosome fracture and the formation of apoptotic bodies [51,52]. In apoptosis caused by exposure to mycotoxins, mitochondrial-mediated apoptosis is the main pathway, which is activated programmed cell death by ROS via mediated by mycotoxins [53]. The mitochondria are an important source of ROS within most mammalian cells [54]. In response to apoptotic stimuli, DNA damage and oxidative stress occur, and eventually the mitochondrial pathway is triggered [30]. The mitochondrial outer membrane is highly permeability in mitochondria [31,55]. Indeed, a previous study reported that when cells are poisoned or subjected to other stimuli, the $\Delta\Psi_m$ decreases [56]. The $\Delta\Psi_m$ disruption is an important trigger in managing apoptosis [57]. Studies have found that ZEN may cause mitochondrial membrane hyperpolarization over a short period of time, followed by loss of the $\Delta\Psi_m$ [58,59]. Previous in vitro experiments demonstrate that ZEN directly causes apoptosis through the mitochondrial pathway at

low concentrations. Subsequently, numerous studies show that ZEN causes intracellular ROS and MDA levels to rise and $\Delta\Psi_m$ decreases, leading to cell apoptosis [32,60,61]. Based on these findings, to reveal whether ZEN-induced apoptosis involves $\Delta\Psi_m$, our study focused on detecting $\Delta\Psi_m$ in SIEC02 cells by JC-1 fluorescence to detect changes in membrane potential. Green fluorescence is indicative of the $\Delta\Psi_m$ decline by JC-1 staining [62,63]. Our results showed that treatment with ZEN caused an increase in ROS and loss of $\Delta\Psi_m$, suggesting that ZEN passed the mitochondrial-mediated pathway. In this study, the percentage of ZEN cells with green fluorescence increased by NAC. This may be because NAC is deacetylated to cysteine, rapidly oxidized, and then transported to cells, which is reduced to GSH, thereby restoring the cell state [6]. The results showed that after addition of NAC pretreatment, $\Delta\Psi_m$ increased, inhibiting apoptosis in SIEC02 cells. This result is consistent with recent studies that have promoted apoptosis of the mitochondria-mediated pathway through ZEN [64].

When mitochondrial membrane permeability changes, cyto c is first released from the mitochondrial membrane space into the cytoplasm, resulting in subsequent activation of caspase-9 [65,66]. Next, activation of caspase-9 activates the downstream performer (caspase-3), thereby triggering apoptosis in the cascade [67]. In the mitochondrial apoptosis pathway, caspase-9 is a key activator of the caspase cascade; caspase-3 is located downstream of the apoptotic ordered cascade reaction and it is the key executor of the transfer, and its activation marks the process of apoptosis [68,69]. Previous studies have found that the production of ROS can proceed from the release of cyto c [70]. Furthermore, a study has shown that ROS can further release cyto c from the mitochondria into the cytoplasm [64]. In this experiment, after ZEN exposure, both intracellular ROS and cyto c increased significantly consistent with previous studies. The Bcl-2 protein family may regulate mitochondrial permeability through both permeabilization of the mitochondrial membrane or translocation of cyto c [28]. Bax is the representative of apoptosis-promoting proteins, and Bcl-2 is a gene that inhibits apoptosis [71]. When the cell damage is serious, Bcl-2 protein expression decreases and Bax protein expression increases [72]. The current study showed that ZEN downregulated Bcl-2 and upregulated Bax mRNA expression, which triggered apoptosis in SIEC02 cells. In the current study, our results showed that after treatment with ZEN toxins, a significant increase in apoptosis was observed. ZEN treatment upregulated mRNA expression of cyto c, caspase-3, and caspase-9. According to the results of this experiment, pretreatment with NAC could inhibit the expression of proapoptotic genes in cells, increase the expression of antiapoptotic genes, and reduce the cell damage induced by ZEN.

4. Conclusions

In conclusion, the results of this study suggested that ZEN induced oxidative stress in SIEC02 cells and sequentially promoted apoptosis through the mitochondrial pathway. ZEN produced substantial cytotoxicity to SIEC02 cells because of elevated ROS levels, which in turn led to increased caspase-3 activation and apoptosis. In addition, NAC pretreatment increased antioxidant enzyme activity, elevated $\Delta\Psi_m$, and inhibited ZEN-induced apoptosis through the mitochondrial pathway. Based on these results, this study provides new insights into the mechanism of action of ZEN on intestinal cells *in vitro*, and the mitigation of this effect by pretreatment with NAC. However, all of the effects of ZEN and its protective mechanisms for the intestine are still not fully understood, and further research is needed.

5. Materials and Methods

5.1. Chemicals and Reagents

ZEN and NAC were supplied by Sigma-Aldrich (St. Louis, MO, USA). Dulbecco modified Eagle medium (DMEM)-F:12 cell culture medium was purchased from Thermo Fisher (Hyclone, Shanghai, China). Fetal bovine serum (FBS) was supplied by Gibco (Invitrogen Corporation, Grand Island, NY, USA). CCK-8 was supplied by Dojindo (Kumamoto, Japan). ROS assay kit, MDA, Gpx, and GR antioxidant kits, and $\Delta\Psi_m$ assay kit with JC-1 were supplied by Beyotime Biotechnology (Nantong,

China). Phosphate buffered saline (PBS) was purchased from Biotopped (Beijing, China). Ethanol at a concentration of 0.25% was chosen as an organic solvent for the dilution of ZEN pure product for subsequent testing.

5.2. Cell Culture and Conditions

SIEC02 cells were donated by Northwest A&F University. The SIEC02 cell line was derived from the mid-jejunum of neonatal, un-suckled, and 1-day-old Landrace piglets [73]. Cells (passages 15–30) were grown in DMEM-F:12 supplemented with 10% fetal calf serum, and 1% penicillin and streptomycin, and cultured at 37 °C in an atmosphere of 5% CO₂ in a cell incubator. The cells were inoculated in a 25 cm² cell culture flask (Nest, Eimer Biotechnology Company, Wuxi, China), and the culture medium was changed after 24 h. When the cells were confluent to approximately 80%–90%, the cell monolayer was washed with PBS and digested with 1 × trypsin/EDTA (Beyotime Institute of Biotechnology, Nantong, China) for subsequent testing.

5.3. Cell Viability Assay

The cytotoxicity of ZEN on SIEC02 cells was measured by CCK-8. Cells ($0.5\text{--}0.8 \times 10^6/\text{mL}$) were seeded in 96-well culture plates for 24 h (Nest, Eimer Biotechnology Company, Wuxi, China) and then treated with ZEN (0, 5, 10, 15, 20, 25 and 30 µg/mL). Similarly, cells were seeded in the same culture plates (6, 12, and 24 h) and then treated with NAC (81, 162, and 324 µg/mL). After all treatments were completed, cells were washed twice with PBS. CCK-8 was then added to a final concentration of 10% in a serum-free medium and cultured at 37 °C for 3 h. The viability rate was measured by measuring the absorbance on a microplate reader with an emission wavelength of 450 nm (SpectraMax M5, Molecular Devices, Sunnyvale, CA, USA).

5.4. Experiment Design

For all experiments, cells were used at 80%–90% confluence and assigned into five treatment groups: control group (cells were incubated with FBS-DMEM-F:12 culture medium for 24 h); ZEN group (cells were incubated with 20 µg/mL ZEN for 24 h); NAC+ZEN group after cells were pretreated with NAC (81, 162 and 324 µg/mL) for 6 h, then placed with fresh culture medium containing 20 µg/mL ZEN for 24 h. The cells of the subsequent experiments ($0.5\text{--}0.8 \times 10^6/\text{mL}$) were seeded in 6-well culture plates (Nest, Eimer Biotechnology Company, Wuxi, China) and treated with drugs as described in this section.

5.5. Determination of Antioxidant Enzyme Activity and Oxidative Products

SIEC02 cells were used for the analysis of antioxidative enzyme and related products. Briefly, cells were washed with 4 °C precooled PBS and resuspended, then lysed on ice. Antioxidant enzyme activities such as Gpx and GR were measured using the assay kit according to the manufacturer's instructions. The results were expressed as µmol/mg or U/mg of protein, respectively. The level of MDA was measured according to the kit instructions, and the results were expressed as nmol/mg of protein. The density of each protein was detected by Enhanced BCA Protein Assay Kit (Beyotime Institute of Biotechnology, Nantong, China).

5.6. Detection of ROS Generation

The balance between the generation and clearance of ROS is important to maintain intracellular redox states. A flow cytometry technique was used to assess the intracellular amounts of ROS with dichlorofluorescein diacetate (DCFH-DA). Briefly, cells were washed with PBS and incubated with 10 µM DCFH-DA at 37 °C for 20 min. After incubated, cells were washed thrice with serum-free cell culture medium. Intracellular production of ROS was measured by a FACS flow cytometry (Becton-Dickinson, San Jose, CA, USA) with an excitation wavelength of 488 nm and an emission

wavelength of 525 nm. The DCF fluorescence intensity indicates the amount of intracellular ROS and the results were analyzed by mean fluorescent intensity (MFI).

5.7. Apoptosis Detection

5.7.1. Annexin V-FITC/PI Double Staining

The apoptosis of SIEC02 cells was measured by the Annexin V-FITC/PI apoptosis detection kit (Biosea Biochemicals, Shanghai, China). Briefly, cells were trypsinized and harvested via centrifugation at $2000\times g$ and $4\text{ }^{\circ}\text{C}$ for 5 min, then re-suspended in 500 μL binding buffer. Annexin-FITC (10 μL) was injected into the solutions and incubated for 40 min at $37\text{ }^{\circ}\text{C}$ in the dark. Finally, 5 μL PI (10 $\mu\text{g}/\text{mL}$) was added. Scattering signals were detected by FACS flow cytometry as described in the previous section.

5.7.2. $\Delta\Psi\text{m}$ Assay

In this experiment, $\Delta\Psi\text{m}$ was monitored by the cationic dye JC-1. Briefly, after treatment and washing three times with PBS, culture medium (1 mL) and JC-1 staining solution (1 mL) are added; after being fully mixed, the cells are incubated at $37\text{ }^{\circ}\text{C}$ for 20 minutes. During incubation, according to 1 mL JC-1 staining buffer ($5\times$) with 4 mL distilled water, JC-1 staining is mixed with JC-1 staining buffer ($1\times$). An increase in the green/red fluorescence intensity ratio indicates mitochondrial membrane depolarization. To each well, 0.5 mL culture medium was added, and the results were detected using a laser scanning confocal microscope (LEICA, Hesse, Germany).

5.7.3. RNA Extraction and Quantitative real time polymerase chain reaction (qRT-PCR)

Total RNA was extracted using RNA fast 200 (Fastagen, Shanghai, China), according to the manufacturer's instruction. The A_{260}/A_{280} ratio was measured by using a Nano Photometer P-Class (Implen GmbH, Munich, Germany) to ensure the purity of the RNA sample, and agarose gel electrophoresis was used to ensure the integrity of the total RNA sample. The complementary DNA (cDNA) was amplified by qRT-PCR using a SYBR Premix Ex Taq RT-PCR kit (Takara, Dalian, China) and used for RT-PCR. SYBR Green I RT-PCR kit (Takara, Dalian, China) was used to measure the mRNA expression of apoptosis-related genes (Bcl-2, Bax, cyto c, caspase-9, caspase-3), and β -actin was used as the internal control gene to correct for differences. The sequences of the specific primers used were as follows in Table 1 [49]. The sequences of the specific primers in this study used were designed from published GenBank sequences, and they were synthesized by Sangon (Shanghai, China).

Table 1. Primers used for qRT-PCR.

Genes	Accession Number	Orientation	Sequences (5'→3')	Fragments Size (bp)	Tm ($^{\circ}\text{C}$)
β -actin	AY550069	Forward	ATGCTTCTAGGCGGACTGT	211	58.2
		Reverse	CCATCCAACCGACTGCT		
Bcl-2	AB271960.1	Forward	GCGACTTTGCCGAGATGT	116	55.9
		Reverse	CACAATCCTCCCCAGTTC		
Bax	XM_003127290.3	Forward	TTTGCTTCAGGGTTTCATCC	113	54.4
		Reverse	GACTACTCGCTCAACTTCTTGG		
Cyto c	NM_001129970.1	Forward	CTCTTACACAGATGCCAACAA	139	56.1
		Reverse	TTCCCTTCTCCCTTCTTCT		
Caspase-9	XM_013998997.1	Forward	GGACATTGGTCTGAGGAGGATT	116	52.3
		Reverse	TGTTGATGATGAGGCAGTGG		
Caspase-3	NM_214131.1	Forward	GACTACTCGCTCAACTTCTTGG	121	54.5
		Reverse	TTGGAAGTGTGGGATTGAGAC		

RT-PCR was performed by an ABI PRISM 7500 SDS thermal cycler (Applied Biosystems, Foster City, CA, USA). The reaction was carried out using a 10 μL system of PCR, including 1.0 μL of cDNA and 0.2 μL of each primer. The cycle numbers and annealing temperature were optimized for each

primer pair. The PCR cycling conditions were as follows: a denaturation step at 95 °C for 30 s, followed by 40 cycles of denaturing at 95 °C for 5 s and annealing at 60 °C for 34 s. The relative expression of the apoptosis cytokine mRNA was measured by the $2^{-\Delta\Delta C_t}$ method [74].

5.8. Statistical Analysis

Data were analyzed using SPSS 17.0 software (SPSS Inc., Chicago, IL, USA, 2008), and the data of three independent experiments were expressed as mean \pm standard deviation (SD). All the experimental data were analyzed for variance uniformity. When the variance was uniform, data were analyzed by a one-way ANOVA followed by Least-Significant Difference (LSD). When the variance was uneven, data were converted into logarithms, and then analyzed by one-way ANOVA followed by LSD. The significance was considered to be at the probability level of $P < 0.05$.

Author Contributions: Conceptualization, J.L.; Data curation, J.W., W.Z., and A.G.; Formal analysis, J.W. and M.L.; Funding acquisition, J.L. and A.S.; Investigation, J.L.; Methodology, J.W. and M.L.; Project administration, J.L.; Software, W.Z. and J.D.; Supervision, J.L. and A.S.; Writing—original draft, J.W. and M.L.; Writing—review & editing, J.L.

Funding: This research was funded by the National Key R&D Program (2016YFD0501207), the Natural Science Foundation of Heilongjiang Province of China (LC2018007), and the China Agriculture Research System (CARS-35).

Conflicts of Interest: The authors declare no conflict of interest.

References

- Rui, G.; Meng, Q.; Li, J.; Min, L.; Zhang, Y.; Bi, C.; Shan, A. Modified halloysite nanotubes reduce the toxic effects of zearalenone in gestating sows on growth and muscle development of their offsprings. *J. Anim. Sci. Biotechnol.* **2016**, *7*, 570–578.
- Gao, X.; Sun, L.; Zhang, N.; Li, C.; Zhang, J.; Xiao, Z.; Qi, D. Gestational zearalenone exposure causes reproductive and developmental toxicity in pregnant rats and female offspring. *Toxins* **2017**, *9*, 21. [[CrossRef](#)] [[PubMed](#)]
- Wu, L.; Li, J.; Li, Y.; Li, T.; He, Q.; Tang, Y.; Liu, H.; Su, Y.; Yin, Y.; Liao, P. Aflatoxin b1, zearalenone and deoxynivalenol in feed ingredients and complete feed from different province in china. *J. Anim. Sci. Biotechnol.* **2016**, *7*, 63. [[CrossRef](#)] [[PubMed](#)]
- Moretti, A.; Logrieco, A.F.; Susca, A. Mycotoxins: An underhand food problem. In *Mycotoxigenic Fungi*; Moretti, A., Susca, A., Eds.; Humana Press: New York, NY, USA, 2017; Volume 1542, pp. 3–12.
- Stanciu, O.; Banc, R.; Cozma, A.; Filip, L.; Miere, D.; Mañes, J.; Loghin, F. Occurrence of fusarium mycotoxins in wheat from europe—a review. *Acta. Universitatis. Cibiniensis.* **2015**, *19*, 35–60. [[CrossRef](#)]
- Venkataramana, M.; Nayaka, S.C.; Anand, T.; Rajesh, R.; Aiyaz, M.; Divakara, S.T.; Murali, H.S.; Prakash, H.S.; Rao, P.V.L. Zearalenone induced toxicity in shsy-5y cells: The role of oxidative stress evidenced by n-acetyl cysteine. *Food Chem. Toxicol.* **2014**, *65*, 335–342. [[CrossRef](#)] [[PubMed](#)]
- Pietsch, C.; Noser, J.; Wettstein, F.E.; Burkhardt-Holm, P. Unraveling the mechanisms involved in zearalenone-mediated toxicity in permanent fish cell cultures. *Toxicon* **2014**, *88*, 44–61. [[CrossRef](#)] [[PubMed](#)]
- Sun, X.D.; Su, P.; Shan, H. Mycotoxin contamination of maize in china. *Compr. Rev. Food Sci. F.* **2017**, *16*, 835–849. [[CrossRef](#)]
- Knutsen, H.K.; Alexander, J.; Barregård, L.; Bignami, M.; Brüschweiler, B.; Ceccatelli, S.; Cottrill, B.; Dinovi, M.; Edler, L.; Grasl-Kraupp, B. Risks for animal health related to the presence of zearalenone and its modified forms in feed. *EFSA J.* **2017**, *15*, e04851.
- Pinton, P.; Nougayrede, J.P.; Del Rio, J.C. The food contaminant deoxynivalenol, decreases intestinal barrier permeability and reduces claudin expression. *Toxicol. Appl. Pharm.* **2009**, *237*, 41–48. [[CrossRef](#)] [[PubMed](#)]
- Goossens, J.; Pasmans, F.; Verbrugghe, E.; Vandenbroucke, V.; De Baere, S.; Meyer, E.; Haesebrouck, F.; De Backer, P.; Croubels, S. Porcine intestinal epithelial barrier disruption by the fusarium mycotoxins deoxynivalenol and T-2 toxin promotes transepithelial passage of doxycycline and paromomycin. *BMC Vet. Res.* **2012**, *8*, 245. [[CrossRef](#)] [[PubMed](#)]
- Tatay, E.; Font, G.; Ruiz, M.J. Cytotoxic effects of zearalenone and its metabolites and antioxidant cell defense in cho-k1 cells. *Food Chem. Toxicol.* **2016**, *96*, 43–49. [[CrossRef](#)] [[PubMed](#)]

13. Marin, D.E.; Taranu, I.; Pistol, G.; Stancu, M. Effects of zearalenone and its metabolites on the swine epithelial intestinal cell line: Ipec 1. *Proc. Nutr. Soc.* **2013**, *72*, 85–89. [[CrossRef](#)]
14. Liu, M.; Gao, R.; Meng, Q.; Zhang, Y.; Bi, C.; Shan, A. Toxic effects of maternal zearalenone exposure on intestinal oxidative stress, barrier function, immunological and morphological changes in rats. *PLoS ONE* **2014**, *9*, e106412. [[CrossRef](#)] [[PubMed](#)]
15. Cortinovis, C.; Caloni, F.; Schreiber, N.B.; Spicer, L.J. Effects of fumonisin b1 alone and combined with deoxynivalenol or zearalenone on porcine granulosa cell proliferation and steroid production. *Theriogenology*. **2014**, *81*, 1042–1049. [[CrossRef](#)] [[PubMed](#)]
16. Hassen, W.; Ayedboussema, I.; Oscoz, A.A.; Lopez, A.C.; Bacha, H. The role of oxidative stress in zearalenone-mediated toxicity in hep g2 cells: Oxidative DNA damage, glutathione depletion and stress proteins induction. *Toxicology* **2007**, *232*, 294–302. [[CrossRef](#)] [[PubMed](#)]
17. Zhu, L.; Yuan, H.; Guo, C.; Lu, Y.; Deng, S.; Yang, Y.; Wei, Q.; Wen, L.; He, Z. Zearalenone induces apoptosis and necrosis in porcine granulosa cells via a caspase-3- and caspase-9-dependent mitochondrial signaling pathway. *J. Cell. Physiol.* **2012**, *227*, 1814–1820. [[CrossRef](#)] [[PubMed](#)]
18. Ayed-Boussema, I.; Bouaziz, C.; Rjiba, K.; Valenti, K.; Laporte, F.; Bacha, H.; Hassen, W. The mycotoxin zearalenone induces apoptosis in human hepatocytes (hepg2) via p53-dependent mitochondrial signaling pathway. *Toxicol. in Vitro* **2008**, *22*, 1671–1680. [[CrossRef](#)] [[PubMed](#)]
19. Schneider, R., Jr.; Santos, C.F.; Clarimundo, V.; Dalmaz, C.; Elisabetsky, E.; Gomez, R. N-acetylcysteine prevents behavioral and biochemical changes induced by alcohol cessation in rats. *Alcohol* **2015**, *49*, 259–263.
20. Wang, W.; Dan, L.; Ding, X.; Zhao, Q.; Chen, J.; Tian, K.; Yang, Q.; Lu, L. N-acetylcysteine protects inner ear hair cells and spiral ganglion neurons from manganese exposure by regulating ros levels. *Toxicol. Lett.* **2017**, *279*, 77–86. [[CrossRef](#)] [[PubMed](#)]
21. Aruoma, O.I.; Halliwell, B.; Hoey, B.M.; Butler, J. The antioxidant action of n-acetylcysteine: Its reaction with hydrogen peroxide, hydroxyl radical, superoxide, and hypochlorous acid. *Free Radical Biol. Med.* **1989**, *6*, 593–597. [[CrossRef](#)]
22. Moreira, M.A.; Irigoyen, M.C.; Saad, K.R.; Saad, P.F.; Koike, M.K.; Montero, E.F.; Martins, J.L. N-acetylcysteine reduces the renal oxidative stress and apoptosis induced by hemorrhagic shock. *J. Surg. Res.* **2016**, *203*, 113–120. [[CrossRef](#)] [[PubMed](#)]
23. Halasi, M.; Wang, M.; Chavan, T.S.; Gaponenko, V.; Hay, N.; Gartel, A.L. Ros inhibitor n-acetyl-l-cysteine antagonizes the activity of proteasome inhibitors. *Biochem. J.* **2013**, *454*, 201–208. [[CrossRef](#)] [[PubMed](#)]
24. Cazzola, M.; Calzetta, L.; Facciolo, F.; Rogliani, P.; Matera, M.G. Pharmacological investigation on the anti-oxidant and anti-inflammatory activity of n-acetylcysteine in an ex vivo model of copd exacerbation. *Resp. Res.* **2017**, *18*, 26. [[CrossRef](#)] [[PubMed](#)]
25. Xue, C.; Liu, W.; Wu, J.; Yang, X.; Xu, H. Chemoprotective effect of n-acetylcysteine (nac) on cellular oxidative damages and apoptosis induced by nano titanium dioxide under uva irradiation. *Toxicol. in Vitro* **2011**, *25*, 110. [[CrossRef](#)] [[PubMed](#)]
26. Sharma, M.; Kaur, T.; Singla, S.K. Role of mitochondria and nadph oxidase derived reactive oxygen species in hyperoxaluria induced nephrolithiasis: Therapeutic intervention with combinatorial therapy of n-acetyl cysteine and apocynin. *Mitochondrion* **2016**, *27*, 15–24. [[CrossRef](#)] [[PubMed](#)]
27. Kondakçı, G.; Aydın, A.F.; Dođru-Abbasođlu, S.; Uysal, M. The effect of n-acetylcysteine supplementation on serum homocysteine levels and hepatic and renal oxidative stress in homocysteine thiolactone-treated rats. *Arch. Physiol. Biochem.* **2017**, *123*, 128–133. [[CrossRef](#)] [[PubMed](#)]
28. Wang, Y.; Zheng, W.; Bian, X.; Yuan, Y.; Gu, J.; Liu, X.; Liu, Z.; Bian, J. Zearalenone induces apoptosis and cytoprotective autophagy in primary leydig cells. *Toxicol. Lett.* **2014**, *226*, 182–191. [[CrossRef](#)] [[PubMed](#)]
29. Thannickal, V.J.; Fanburg, B.L. Reactive oxygen species in cell signaling. *Am. J. Physiol. Lung Cell. Mol. Physiol.* **2000**, *279*, L1005. [[CrossRef](#)] [[PubMed](#)]
30. Prosperini, A.; Juan-García, A.; Font, G.; Ruiz, M.J. Beauvericin-induced cytotoxicity via ros production and mitochondrial damage in caco-2 cells. *Toxicol. Lett.* **2013**, *222*, 204–211. [[CrossRef](#)] [[PubMed](#)]
31. Wu, J.; Jing, L.; Yuan, H.; Peng, S.-q. T-2 toxin induces apoptosis in ovarian granulosa cells of rats through reactive oxygen species-mediated mitochondrial pathway. *Toxicol. Lett.* **2011**, *202*, 168–177. [[CrossRef](#)] [[PubMed](#)]

32. Tatay, E.; Espín, S.; Garcíafernández, A.J.; Ruiz, M.J. Oxidative damage and disturbance of antioxidant capacity by zearalenone and its metabolites in human cells. *Toxicol. in Vitro* **2017**, *45*, 334. [[CrossRef](#)] [[PubMed](#)]
33. Bensassi, F.; Gallerne, C.; Sharaf el Dein, O.; Hajlaoui, M.R.; Lemaire, C.; Bacha, H. In vitro investigation of toxicological interactions between the fusariotoxins deoxynivalenol and zearalenone. *Toxicon* **2014**, *84*, 1–6. [[CrossRef](#)] [[PubMed](#)]
34. Cornelia, B.; Sonia, S.; Roxana, C.P.; Raduly, L.; Ovidiu, B.; Ionelia, T.; Eliza, M.D.; Monica, M.; Ancuta, J.; Patriciu, A.C. Evaluation of cellular and molecular impact of zearalenone and ochratoxin A exposure on ipec-1 cells using microarray technology. *BMC Genomics* **2016**, *17*, 576.
35. Wan, L.Y.; Turner, P.C.; Elnezami, H. Individual and combined cytotoxic effects of fusarium toxins (deoxynivalenol, nivalenol, zearalenone and fumonisins b1) on swine jejunal epithelial cells. *Food Chem. Toxicol.* **2013**, *57*, 276–283. [[CrossRef](#)] [[PubMed](#)]
36. Ferrer, E.; Juangarcía, A.; Font, G.; Ruiz, M.J. Reactive oxygen species induced by beauvericin, patulin and zearalenone in CHO-K1 cells. *Toxicol. in Vitro* **2009**, *23*, 1504–1509. [[CrossRef](#)] [[PubMed](#)]
37. Kang, C.; Lee, H.; Yoo, Y.S.; Hah, D.Y.; Kim, C.H.; Kim, E.; Kim, J.S. Evaluation of oxidative DNA damage using an alkaline single cell gel electrophoresis (scge) comet assay, and the protective effects of n-acetylcysteine amide on zearalenone-induced cytotoxicity in Chang liver cells. *Toxicol. Res.* **2013**, *29*, 43–52. [[CrossRef](#)] [[PubMed](#)]
38. Birben, E.; Sahiner, U.M.; Sackesen, C.; Erzurum, S.; Kalayci, O. Oxidative stress and antioxidant defense. *World Allergy Organ. J.* **2012**, *5*, 9–19. [[CrossRef](#)] [[PubMed](#)]
39. Pundir, M.; Arora, S.; Kaur, T.; Singh, R.; Singh, A.P. Effect of modulating the allosteric sites of N-methyl-D-aspartate receptors in ischemia-reperfusion induced acute kidney injury. *J. Surg. Res.* **2013**, *183*, 668–677. [[CrossRef](#)] [[PubMed](#)]
40. Yan, S.H.; Wang, J.H.; Zhu, L.S.; Chen, A.M.; Wang, J. Thiamethoxam induces oxidative stress and antioxidant response in zebrafish (*Danio rerio*) livers. *Environ. Toxicol.* **2016**, *31*, 2006–2015. [[CrossRef](#)] [[PubMed](#)]
41. Abid, E.S.; Ee, B.C.B. Comparative study of toxic effects of zearalenone and its two major metabolites alpha-zearalenol and beta-zearalenol on cultured human Caco-2 cells. *J. Biochem. Mol. Toxicol.* **2009**, *23*, 233–243. [[CrossRef](#)] [[PubMed](#)]
42. Fan, W.; Shen, T.; Ding, Q.; Lv, Y.; Li, L.; Huang, K.; Yan, L.; Song, S. Zearalenone induces ROS-mediated mitochondrial damage in porcine iPEC-J2 cells. *J. Biochem. Mol. Toxicol.* **2017**, *31*, e21944. [[CrossRef](#)] [[PubMed](#)]
43. Dennog, C.; Radermacher, P.; Barnett, Y.A.; Speit, G. Antioxidant status in humans after exposure to hyperbaric oxygen. *Mutat. Res.* **1999**, *428*, 83–89. [[CrossRef](#)]
44. Phamhuy, L.A.; He, H.; Phamhuy, C. Free radicals, antioxidants in disease and health. *Int. J. Biomed. Sci.* **2008**, *4*, 89–96.
45. Assady, M.; Farahnak, A.; Golestani, A.; Esharghian, M. Superoxide dismutase (SOD) enzyme activity assay in *Fasciola* spp. parasites and liver tissue extract. *Iran. J. Parasitol.* **2011**, *6*, 17. [[PubMed](#)]
46. Wu, G.; Fang, Y.Z.; Yang, S.; Lupton, J.R.; Turner, N.D. Glutathione metabolism and its implications for health. *J. Nutr.* **2004**, *134*, 489. [[CrossRef](#)] [[PubMed](#)]
47. Ashrafzadeh, T.H.; Saeed, H.; Foad, R.; Ashrafzadeh, T.M.; Hadi, H. Effects of n-acetylcysteine and pentoxifylline on remote lung injury in a rat model of hind-limb ischemia/reperfusion injury. *J. Bras. Pneumol.* **2016**, *42*, 9.
48. Nazıroğlu, M.; Şenol, N.; Ghazizadeh, V.; Yürüker, V. Neuroprotection induced by n-acetylcysteine and selenium against traumatic brain injury-induced apoptosis and calcium entry in hippocampus of rat. *Cell Mol. Neurobiol.* **2014**, *34*, 895. [[CrossRef](#)] [[PubMed](#)]
49. Wei, Z.; Zhang, S.; Zhang, M.; Yang, L.; Cheng, B.; Li, J.; Shan, A. Individual and combined effects of fusarium toxins on apoptosis in PK15 cells and the protective role of n-acetylcysteine. *Food Chem. Toxicol.* **2017**, *111*, 27–43.
50. Yeo, E.H.; Goh, W.L.; Chow, S.C. The aminopeptidase inhibitor, Z-L-CMK is toxic and induced cell death in Jurkat T cells through oxidative stress. *Toxicol. Mech. Methods.* **2017**, *28*, 157–166. [[CrossRef](#)] [[PubMed](#)]
51. Zhao, J.; Kyotani, Y.; Itoh, S.; Nakayama, H.; Isosaki, M.; Yoshizumi, M. Big mitogen-activated protein kinase 1 protects cultured rat aortic smooth muscle cells from oxidative damage. *J. Pharmacol. Sci.* **2011**, *116*, 173–180. [[CrossRef](#)] [[PubMed](#)]
52. Hotchkiss, R.S.; Strasser, A.; McDunn, J.E.; Swanson, P.E. Cell death. *N. Engl. J. Med.* **2009**, *361*, 1570–1583. [[CrossRef](#)] [[PubMed](#)]

53. Borys, S.; Khozmi, R.; Kranc, W.; Bryja, A.; Dyszkiewiczkonwińska, M.; Jeseta, M.; Kempisty, B. Recent findings of the types of programmed cell death. *Adv. Cell Biol.* **2017**, *5*, 43–49. [[CrossRef](#)]
54. Murphy, M.P. How mitochondria produce reactive oxygen species. *Biochem. J.* **2009**, *417*, 1–13. [[CrossRef](#)] [[PubMed](#)]
55. Guo, Z.Y.; Xu, M.H.; He, W.; Wang, S.T.; Guo, Z.Y.; Xu, M.H.; He, W.; Wang, S.T. Effect of mitochondria permeability transition pore on h9c2 myocardial cell apoptosis induced by lipopolysaccharide. *J. Shanghai Jiaotong Univ.* **2017**, *37*, 942–949.
56. Vaca, C.E.; Wilhelm, J.; Harms-Ringdahl, M. Interaction of lipid peroxidation products with DNA. A review. *Mutat. Res.* **1988**, *195*, 137–149. [[CrossRef](#)]
57. Hüttemann, M.; Pecina, P.; Rainbolt, M.; Sanderson, T.H.; Kagan, V.E.; Samavati, L.; Doan, J.W.; Lee, I. The multiple functions of cytochrome c and their regulation in life and death decisions of the mammalian cell: From respiration to apoptosis. *Mitochondrion* **2011**, *11*, 369–381. [[CrossRef](#)] [[PubMed](#)]
58. Bras, M.; Queenan, B.; Susin, S.A. Programmed cell death via mitochondria: Different modes of dying. *Biochemistry (Moscow)* **2005**, *70*, 231–239. [[CrossRef](#)]
59. Leal, A.M.D.S.; Queiroz, J.D.F.D.; Lima, T.K.D.S.; Agnezlina, L.F. Violacein induces cell death by triggering mitochondrial membrane hyperpolarization in vitro. *BMC Microbiol.* **2015**, *15*, 1–8. [[CrossRef](#)] [[PubMed](#)]
60. Abbès, S.; Salahabbès, J.B.; Ouanes, Z.; Houas, Z.; Othman, O.; Bacha, H.; Abdelwahhab, M.A.; Oueslati, R. Preventive role of phyllosilicate clay on the immunological and biochemical toxicity of zearalenone in balb/c mice. *Int. Immunopharmacol.* **2006**, *6*, 1251–1258. [[CrossRef](#)] [[PubMed](#)]
61. Eraslan, G.; Kanbur, M.; Aslan, Ö.; Karabacak, M. The antioxidant effects of pumpkin seed oil on subacute aflatoxin poisoning in mice. *Environ. Toxicol.* **2013**, *28*, 681–688. [[CrossRef](#)] [[PubMed](#)]
62. Wu, L.L.; Dunning, K.R.; Yang, X.; Russell, D.L.; Norman, R.J.; Robker, R.L. In Oocytes exhibit lipid accumulation, endoplasmic reticulum stress, mitochondrial dysfunction, and apoptosis in response to high fat diet. *Biol. Reprod.* **2010**, *83*, 185. [[CrossRef](#)]
63. Ly, J.D.; Grubb, D.R.; Lawen, A. The mitochondrial membrane potential ($\delta\psi_m$) in apoptosis; an update. *Apoptosis* **2003**, *8*, 115–128. [[CrossRef](#)] [[PubMed](#)]
64. Yun, Y.; Zong, M.; Xu, W.; Yang, Z.; Bo, W.; Yang, M.; Tao, L. Natural pyrethrins induces apoptosis in human hepatocyte cells via bax- and bcl-2-mediated mitochondrial pathway. *Chem. Biol. Interact.* **2017**, *262*, 38–45.
65. Guo, L.; Peng, Y.; Yao, J.; Sui, L.; Gu, A.; Wang, J. Anticancer activity and molecular mechanism of resveratrol-bovine serum albumin nanoparticles on subcutaneously implanted human primary ovarian carcinoma cells in nude mice. *Cancer Biother. Radiopharm.* **2010**, *25*, 471. [[CrossRef](#)] [[PubMed](#)]
66. Tsai, C.H.; Yang, S.H.; Chien, C.M.; Lu, M.C.; Lo, C.S.; Lin, Y.H.; Hu, X.W.; Lin, S.R. Mechanisms of cardiotoxin iii-induced apoptosis in human colorectal cancer colo205 cells. *Clin. Exp. Pharmacol. Physiol.* **2006**, *33*, 177–182. [[CrossRef](#)] [[PubMed](#)]
67. Deng, L.; Ding, D.; Su, J.; Manohar, S.; Salvi, R. Salicylate selectively kills cochlear spiral ganglion neurons by paradoxically up-regulating superoxide. *Neurotox. Res.* **2013**, *24*, 307–319. [[CrossRef](#)] [[PubMed](#)]
68. Hua, P.; Liu, J.; Tao, J.; Liu, J.; Yang, S. Influence of caspase-3 silencing on the proliferation and apoptosis of rat bone marrow mesenchymal stem cells under hypoxia. *Int. J. Clin. Exp. Med.* **2015**, *8*, 1624–1633. [[PubMed](#)]
69. Wang, X.; Diao, Y.; Liu, Y.; Gao, N.; Gao, D.; Wan, Y.; Zhong, J.; Jin, G. Synergistic apoptosis-inducing effect of aspirin and isosorbide mononitrate on human colon cancer cells. *Mol. Med. Rep.* **2015**, *12*, 4750. [[CrossRef](#)] [[PubMed](#)]
70. Vacca, R.A.; Valenti, D.; Bobba, A.; Merafina, R.S.; Passarella, S.; Marra, E. Cytochrome c is released in a reactive oxygen species-dependent manner and is degraded via caspase-like proteases in tobacco bright-yellow 2 cells en route to heat shock-induced cell death. *Plant Physiol.* **2006**, *141*, 208–219. [[CrossRef](#)] [[PubMed](#)]
71. Czabotar, P.E.; Lessene, G.; Strasser, A.; Adams, J.M. Control of apoptosis by the bcl-2 protein family: Implications for physiology and therapy. *Nat. Rev. Mol. Cell Biol.* **2014**, *15*, 49–63. [[CrossRef](#)] [[PubMed](#)]
72. Sun, L.H.; Lei, M.Y.; Zhang, N.Y.; Gao, X.; Li, C.; Krumm, C.S.; Qi, D.S. Individual and combined cytotoxic effects of aflatoxin b1, zearalenone, deoxynivalenol and fumonisin b1 on brl 3a rat liver cells. *Toxicon* **2015**, *95*, 6. [[CrossRef](#)] [[PubMed](#)]

73. Wang, J.; Hu, G.; Lin, Z.; He, L.; Xu, L.; Zhang, Y. Characteristic and functional analysis of a newly established porcine small intestinal epithelial cell line. *PLoS ONE* **2014**, *9*, e110916. [[CrossRef](#)] [[PubMed](#)]
74. Bousquet, L.; Pruvost, A.; Guyot, A.; Farinotti, R.; Mabondzo, A. Combination of tenofovir and emtricitabine plus efavirenz: In vitro modulation of abc transporter and intracellular drug accumulation. *Antimicrob. Agents Chemother.* **2009**, *53*, 896. [[CrossRef](#)] [[PubMed](#)]



© 2018 by the authors. Licensee MDPI, Basel, Switzerland. This article is an open access article distributed under the terms and conditions of the Creative Commons Attribution (CC BY) license (<http://creativecommons.org/licenses/by/4.0/>).